Vol.2, No.3, 74-79 (2013)
http://dx.doi.org/10.4236/ojrm.2013.23011

Open Journal of Regenerative Medicine

Gradients of Al/Al_2O_3 nanostructures for screening mesenchymal stem cell proliferation and differentiation

Michael Veith[1,2*], Cécile Dufloux[2], Soraya Rasi Ghaemi[3], Cenk Aktas[2], Nicolas H. Voelcker[3]

[1]Department of Inorganic Chemistry, Saarland University, Saarbrücken, Germany;
[*]Corresponding Author: michael.veith@inm-gmbh.de
[2]INM—Leibniz Institute for New Materials, CVD/Biosurfaces Group, Saarbrücken, Germany
[3]Mawson Institute, Division of Information Technology, Engineering and the Environment Division Office, Mawson Lakes Campus, University of South Australia, Adelaide, Australia

Received 30 April 2013; revised 5 June 2013; accepted 10 July 2013

ABSTRACT

By decomposing a molecular precursor we fabricated a novel surface based on an aluminium/aluminiumoxide composite incorporating nanotopography gradient to address high-throughput and fast analysis method for studying stem cell differentiation by nanostructures. Depending on the topography of the nanostructures, mesenchymal stem cells exhibit a diverse proliferation and differentiation behavior.

Keywords: Gradient; Nanowires; Stem Cell; Topography

1. INTRODUCTION

Visual cell-substratum interaction is governed by topography in addition to surface chemistry. Especially nanotopography of the surface plays a critical role in accelerating the cell proliferation and enhancing tissue interaction with a reduced immune response [1,2]. Nanoscaled topography may also influence cell morphology, alignment, migration, and proliferation [3]. The proven impact of nanotopography on both basic cell function and gene expression indicates that it might be possible to direct the cell differentiation by the nanostructured surface features, too [4].

Stem cells have the ability to differentiate into various lineages. Controlled stem cell differentiation will have enormous potential for basic research and clinical therapy [5]. Nanotopography is a useful tool for guiding differentiation, as the physical surface patterns are more durable and stable than those obtained by chemical surface modification. In addition, surface patterns can be prepared in different size and shapes as a customized approach to control the differentiation. Several recent studies have investigated the influence of nanotopography on mesenchymal stem cell (MSCs) proliferation and differentiation into specific cell lineages [6,7]. Jin *et al*. showed the differentiation of human mesenchymal stem cells (hMSC) into osteoblasts by altering the dimensions of nano-tubular shaped titanium oxide surface structures [8]. Since no osteogenic inducing media was used in this study, it is obvious that there is a direct effect of the geometric features on the differentiation. Similarly, we have shown that runt-related transcription factor 2 (Runx2), bone sialoprotein (BSP), osteopontin (OPN) and alkaline phosphatase ALP are up-regulated on 1D Al_2O_3 nanostructures and these show the sole effect of the nanotopography on the differentiation [9]. On the other hand, there is a clear need for a more systematic study to understand the effect of the nanotopography on the stem cell proliferation and differentiation. One should think about preparing different surface structures by altering the geometry/shape, distribution density/interspacing and scale/size systematically. Time consuming processing and analysis of several substrates with different surface topographies are the main limitations in studying topography induced differentiation.

Incorporating topographic gradients on a substrate can serve as a high-throughput and fast analysis approach for studying the effect of surface topography on the stem cell differentiation rather than fabrication and analysis of multiple substrates. Actually, inducing physical, chemical, and biological signal gradients into engineered biomaterials is also one of the current approaches to creating a microenvironment which mimics the *in vivo* cellular and tissue complexity [10]. Kunzler *et al*. showed that nanotopography of particle gradients has a significant

influence on cell proliferation and morphology [11]. Previously, we have shown that osteogenesis of rMSCs is enhanced on porous silicon gradient (pore size) compared with flat Si substrates [12]. Although the porosity is counted as a topographic feature, this work cannot be counted as direct nanotopography (shape or morphology) driven differentiation.

Here, we present a novel surface incorporating nanotopography gradient to address high-throughput and fast analysis method for studying stem cell differentiation by nanostructures.

2. EXPERIMENTAL

2.1. Gradient Surface Fabrication

The nanostructures were fabricated by Chemical Vapor Deposition (CVD) of the molecular precursor $\left[H_2Al\left(O^tBu\right)\right]_2$ [14]. The decomposition of this single source precursor is known to lead to different structures, depending on the decomposition temperature. While nanoparticles form at 400˚C, nanowires are observed at a deposition temperature of 500˚C to 600˚C. These nanoparticles as well as the nanowires are composed of an aluminum core and a uniform aluminum oxide shell (completely wrapping-up this core). This temperature driven morphology control is used as the basis for the preparation of gradient topography. A customized low pressure cold-wall CVD apparatus, as already described elsewhere [13] was used. Basically, the substrate holder was heated up to 600˚C by a high-frequency induction system operating at 400 - 450 kHz. The deposition lasted 4 minutes under the steady stream of the precursor at a pressure of 9×10^{-3} mbar. The glass substrate was placed on a specially designed graphite holder. The holder kept the glass substrate 18˚ inclined to the flow axis and only one extremity of glass was kept in direct contact with the graphite holder. The rest of the glass substrate was subjected to precursor flow as free-standing in the chamber. In this way, a temperature gradient was achieved which was monitored by a high-resolution thermal camera (images are not given here). While the bottom-end (which was in direct contact with the graphite holder) reached almost 600˚C, this temperature drops to 400˚C at the free-standing edge of the glass substrate.

2.2. Scanning Electron Microscopy (SEM)

SEM images were taken with high-resolution SEM at an acceleration voltage of 20 kV and a working distance of 9.8 mm. Samples were coated with a thin layer of Au prior to analysis to prevent surface charging.

2.3. Cell Isolation and Culture

The mesenchymal stem cells were harvested from the bone marrow of 100 g Wistar rats (from Animal Care Unit, Flinders University of South Australia). Animals were sacrificed by the guidelines approved by the Animal Welfare Committee to expose femur and tibia bones. Bone marrow was collected by flushing bones with Dulbecco's modified eagle medium (DMEM-low glucose) (Sigma) supplemented with 10% fetal bovine serum (FBS), 0.1 mmol non-essential amino acids and 100 $U \cdot mL^{-1}$ penicillin (Sigma). The cells were then treated with RBC lysis buffer (0.15 mol ammonium chloride, 10 mmol potassium bicarbonate, 0.1 mmol EDTA) for five minutes to remove red blood cells. After washing the cells with medium, cells were re-suspended in complete DMEM then incubated at 37˚C and 5% CO_2. The medium was replaced every two days until the confluence. Only third passage cells were seeded on prepared surfaces.

Prior to incubation of cells, prepared surfaces were washed with 70% ethanol and sterile Dulbecco's PBS, then the slides were sterilized with Antibiotic-Antimycotic 2× (GIBCO) for 4 h. Each gradient surface and a glass slide as a control were placed in 12-well plate (Nunc) and were seeded with cells at the density of 10,000 $cells \cdot cm^{-2}$. The cells were incubated four hours at 37˚C and 5% CO_2, and then unattached cells were removed. Consequently, the cells were incubated in fresh DMEM, including 10% FBS at 37˚C and 5% CO_2 for three or four days before adding the differentiated medium. Meanwhile, the captured cells were counted after 4 h incubation time and 48 h culturing following the staining with fluorescent dyes. Cell viability was also assessed with 15 $\mu g \cdot mL^{-1}$ fluorescein diacetate (FDA) and 10 µmol propodium iodide (PI) (GIBCO) after seven days culturing on the gradient surface.

2.4. Staining and Fluorescence Imaging

The immobilized cells on the surface were labeled with fluorescent dyes then evaluated with a Nikon Eclipse E600 microscope. Tubulin and F-actin in MSC were labeled by phalloidin-tetramethylrhodamine B isothiocyanate (Sigma) (excitation and emission: 540 - 573 nm) and nuclei with Hoechst (Sigma) (excitation and emission: 346 - 460 nm). Briefly, cells were washed with PBS, fixed with 4% paraformaldehyde (Sigma) and permeabilized with 0.25% Triton X-100 (Sigma), then stained with 2 $\mu g \cdot mL^{-1}$ Hoechst (Invitrogen) for 15 minutes at room temperature and 100 µmol Phalloidin for 30 minutes.

2.5. Osteogenic Differentiation Analysis/ Examination of Mineralization on Microarrays

The samples were analyzed for the rate of differentiation to osteogenic lineage at the late stage of differentiation by calcein blue staining. Calcein blue powder (Sigma) was dissolved in 100 mmol KOH at the concentration of 30 $mmol \cdot L^{-1}$ then filtrated. Calcein blue solu-

tion was added into the medium at final concentration of 30 µmol·L^{-1} for overnight. Calcein blue emissions a blue color under fluorescent microscope using a DAPI filter (excitation and emission: 370 - 435 nm). To accelerate differentiation, pre-warmed DMEM including 25 mmol 10% FBS, 10 - 7 mol Dexamethasone, 10 mmol Beta-Glycerol-Phosphate and 50 µg/mL^{-1} Ascorbic Acid Bi-Phosphate was added on top of every slide. The medium was replaced with fresh medium every three days. The cells were cultured over 21 days.

3. RESULTS AND DISCUSSIONS

The obtained surface provides a gradient in morphology varying from zero-dimensional (0D) to one-dimensional (1D) nanostructures. Scanning electron microscopy (SEM) images taken at different positions along the gradient are shown in **Figure 1**.

The highest aspect ratio nanostructures are seen at "position a" on the gradient axis (the region which was exposed to higher deposition temperature). The aspect ratio decreases continuously following the gradient axis towards the less heated end (**Figure 1(c)-(h)**). At the end of the gradient which was not in direct contact with the substrate holder, only spherical 0D nanostructures are present (**Figure 1(h)**). Previously we have shown that all

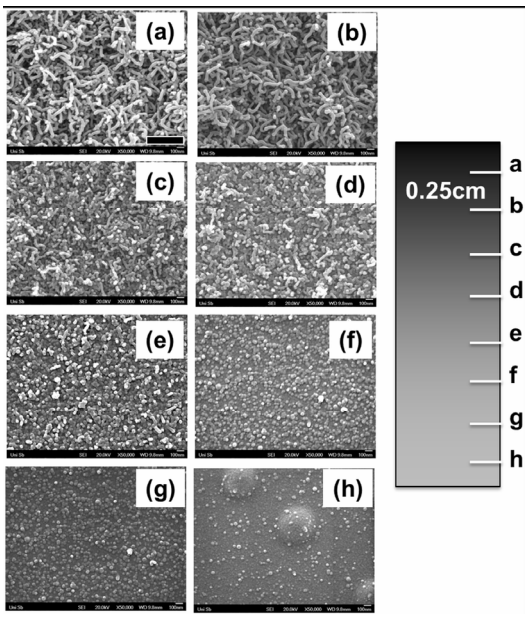

Figure 1. SEM images of different positions on topography gradient (the scale bar corresponds to 400 nm). The different regions on the gradient are indicated in the sketch given at the right side of the figure. Gradients were produced by exposing the substrate to a temperature gradient within a cold-wall CVD reactor. While the regions (a)-(c) were in contact with the graphite holder, the regions (d)-(h) were freely standing in the chamber.

these 0D and 1D nanostructures exhibit the identical surface chemistry. These nanostructures are composed of Al core and Al_2O_3 shell as a result of a disproportionation reaction which we presented previously [14]. We have carried out our several studies on the formation of these nanostructures by altering the deposition temperatures. While nanoparticles form at lower temperatures around 400˚C - 450˚C, nanowires form at higher temperatures (600˚C - 650˚C). In addition, we have shown that at high deposition temperatures, keeping the deposition time longer leads to more tangled and high-aspect ratio 1D nanostructures. Previously, we have shown that these structures exhibit identical surface chemistry [15, 16]. The outer surface of all these structures is made of Al_2O_3 which has been used as bioceramic in various implant applications [13,15].

Our gradient surface acts as an ideal substrate for screening the effect of the surface topography and morphology on the cellular response. In this current work, using MSCs isolated from bone marrow Wistar rats, we observed the morphological changes induced by the surface topography at time points of 4 h and 48 h. While analyzing the cellular response to the surface, the substrate was divided into three main regions as follows: 1D nanostructures, transition nanostructures (between 1D and 0D) and 0D nanostructures. The highest cell density was observed on 0D nanostructures (in regions **(f)-(h)** on the gradient axis shown in **Figure 1**). Moving to the 1D nanostructures regions (**(a)-(c)** in **Figure 1**), there is a clear reduction in the cell density. Over the transition regions (**(d)-(e)** in **Figure 1**), the lowest cell density was observed. In addition to the changes in the cell adhesion density, there are clear differences in phenotypes. In 0D nanostructures region, the cells exhibit a highly expanded morphology with well-organized actin filaments and several branched-filopodia (as seen in **Figure 2**) in comparison to those examined on other regions and on the control substrate. The majority of rMSCs on 1D nanostructures region exhibit very distinct focal adhesion sites. Generally, such sharp focal adhesion sites are indication of a strong cell adhesion. On the other hand, the cytoplasm of cells on this region seems to be not as expanded as it was observed on 0D nanostructures region and even some cells exhibit narrow cytoplasm stretched around the nucleus. On the transitional region (composed of 0D to 1D nanostructures), we observed a drastic decrease in the cell density. In addition, we observed a totally different cell phenotype on the transitional region. There is a clear reduction in focal adhesion sites and the majority of cells have rim-shaped non-uniform cytoplasm morphologies.

After 48 hours culturing period, on 0D nanostructures region we observed that rMSCs spread over larger areas and the proliferation increased. While the transformation

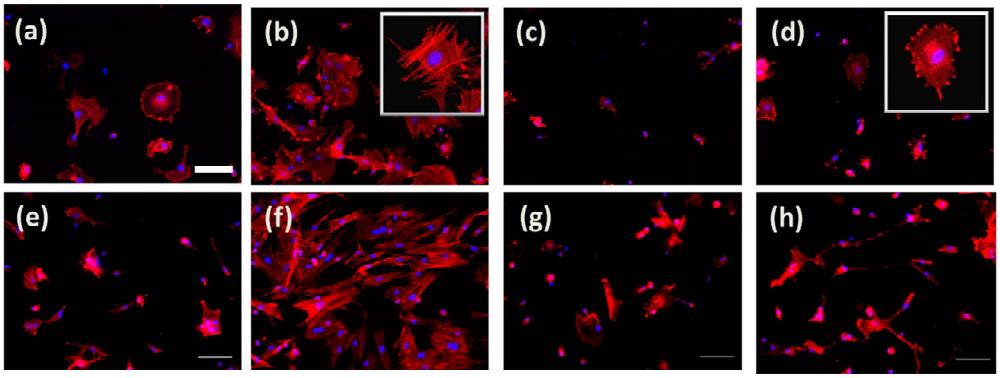

Figure 2. Fluorescence images of cell morphology at different positions of the topography gradient. rMSCs are cultured for 4 h (top images) and 48 h (bottom images). The scale bar is 100 µm (Nucleus: Blue (Hoechst 33342), Cytoplasm: Red (Phalloidin)). (a)-(e) glass control, (b)-(f) 0D nanoparticles region, (c)-(g) transition nanostructures region, and (d)-(h) 1D nanostructures region.

into a more expanded morphology indicates a good cell adhesion, the increased proliferation implies healthy cell growth. Spread cell morphology and distinct actin filaments are supporting cues of a strong cell adhesion. On the other hand, longer culturing period did not lead to an increased cell density and proliferation on 1D nanostructures and transitional region. On 1D nanostructures region, cells exhibit elongated and spindle-shaped cytoplasms (**Figure 2**) indicating a huge alteration in phenotype.

Our quantitative analysis of the cell density shows that even after 4 h culturing period, cells seem well to proliferate on 0D nanostructures region. At a time point of 48 h, one can see a clear difference in the cell densities. While the density of cells on 0D nanostructures is around 189.8% ± 3.7%, this value drops down to 54.3% ± 0.6% in case of transitional nanostructures (see **Figure 3**). Although the cell density of 1D nanostructures is much lower than that of 0D nanostructures, these surfaces enhance the cell adhesion and proliferation with respect to the glass substrate (control). This is a clear indication of cytocompatibility of our surfaces.

These quantitative results show clearly that while rMSCs proliferate well on 0D nanostructures region, somehow the surface topography of 1D nanostructures and transitional regions hinder the growth and proliferation of cells (**Figure 3**). Meanwhile, the presence of 1D nanostructures increased the proliferation rate in comparison to glass substrate (control) and transitional region of the prepared substrate. One of the most striking features of rMSCs analyzed on 1D nanostructures region was that cells prefer to stay beside each other.

Our previous experiences indicate that such changes in the cell morphology can be connected to the differentiation. On the other hand, differentiation needs a more detailed analysis (at the molecular level) of different growth factors and genetic expressions. Recently, we have observed differences in the up regulation of BSP and OPN on 1D nanostructured surfaces [9].

In this current work, we assessed osteogenic differentiation of rMSC on our topography gradient surface. We used calcein blue, which binds to the calcium ion, and considered the resulting fluorescence under ultraviolet light. Overnight incubation of cells stained with 30 µmol of calcein blue resulted in sufficient fluorescence of bone-like nodules on the surface (**Figure 4**). The results showed that there is a significant difference between the 0D nanostructures region and the rest of the surface in terms of the number and size of mineralized nodules (**Figure 4(b)**). Only a few mineralized nodules were observed on the glass on day 21 (**Figure 4(a)**) and these nodules were extremely small to be detected by fluorescence microscopy. In comparison, we observed larger mineralized nodules on the transitional region (**Figure 4(c)**). The number of mineralized nodules and the total area of these nodules obviously increased on the 1D nanostructures region and this might be hint of the differentiation into osteoblast (**Figure 4(d)**). Among other regions, we observed the largest-bone like nodules on 0D nanostructures. At first sight, the clear differences in calcein blue level on different (**Figure 4(e)**) surfaces can be a clear indication of the surface enhanced osteogenesis.

4. CONCLUSION

We showed that the topography gradient by introducing nanostructures (0D to 1D) is an effective tool to screen the adhesion and proliferation of mesenchymal stem cells. Our single source precursor concept leads to a synthesis of nanostructures with different topographies but identical surface chemistry. This forms the basis for studying the sole effect of the topography on the cellular behavior. The effect of the topography gradient on the up-regulation of growth factors and genes will be studied in detail in the future.

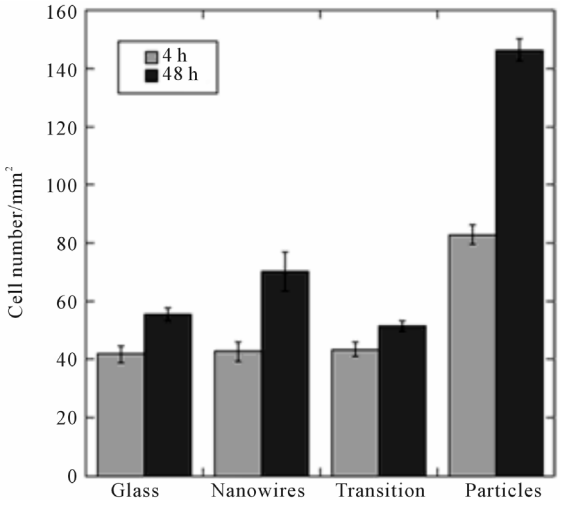

Figure 3. Cell density on different topography (glass control, 0D, transitional and 1D nanostructures regions) at time points of 4 h and 48 h.

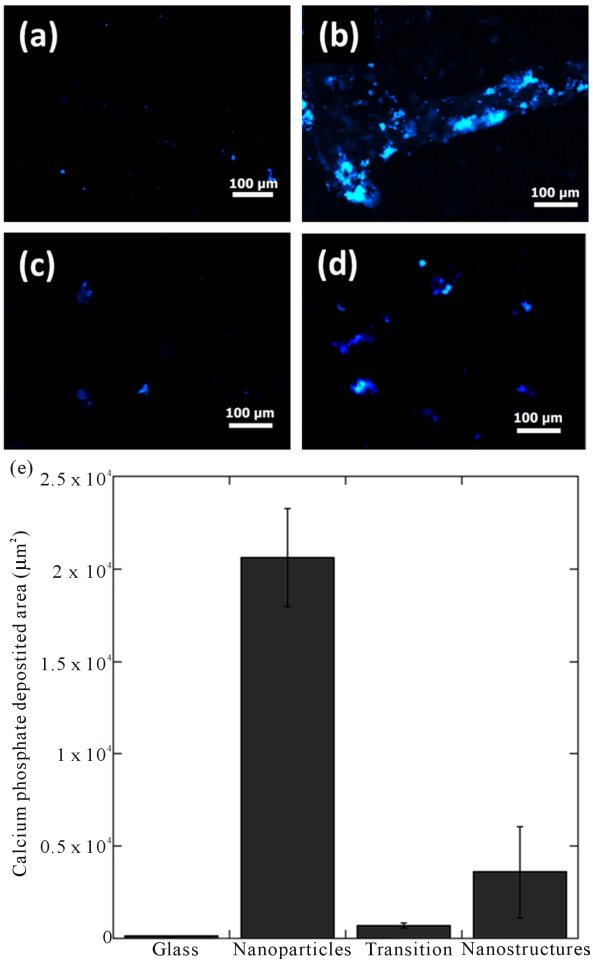

Figure 4. Fluorescence images of differentiated MSCs stained with calcein blue on (a) glass control, (b) 0D nanoparticles region, (c) transitional region, (d) 1D nanostructures regions. (e) Comparison of calcium phosphate deposition on different regions.

5. ACKNOWLEDGEMENTS

We gratefully acknowledge support from bilateral program supported by BMBF (German Ministry of Education and Research) and Australian National Research Foundation under the project number 01DR-12063.

REFERENCES

[1] Jung, D.R., Kapur, R., Adams, T., Giuliano, K.A., Mrksich, M., Craighead, H.G. and Taylor, D.L. (2001) Topographical and physicochemical modification of material surface to enable patterning of living cells. *Critical Reviews in Biotechnology*, **21**, 111-154. doi:10.1080/20013891081700

[2] Oha, S., Brammera, K.S., Lib, Y.S.J., Teng, D., Engler, A.J., Chien, S. and Jina, S. (2008) Stem cell fate dictated solely by altered nanotube dimensions. *Proceedings of the National Academy of Sciences*, **105**, 2307.

[3] Bettinger, C.J., Langer, R. and Borenstein, J.T. (2009) Engineering substrate topography at the micro- and nanoscale to control cell function. *Angewandte Chemie International Edition*, **48**, 5406-5415. doi:10.1002/anie.200805179

[4] Chou, L., Firth, J.D., Uitto, V.J. and Brunette, D.M. (1995) Substratum surface topography alters cell shape and regulates fibronectin mRNA level, mRNA stability, secretion and assembly in human fibroblasts. *Journal of Cell Science*, **108**, 1563.

[5] McNamara, L.E., McMurray, R.J., Biggs, M.J.P., Kantawong, F., Oreffo, R.O.C. and Dalby, M.J. (2010) Nanotopographical control of stem cell differentiation. *Journal of Tissue Engineering*, **1**, 120623. doi:10.4061/2010/120623

[6] Chen, W., Villa-Diaz, L.G., Sun, Y., Weng, S., Kim, J.K., Lam, R.H.W., Han, L., Fan, R., Krebsbach, P.H. and Fu, J. (2012) Nanotopography influences adhesion, spreading, and self-renewal of human embryonic stem cells. *ACS Nano*, **6**, 4094-4103. doi:10.1021/nn3004923

[7] Zouani, O.F., Chanseau, C., Brouillaud, B., Bareille, R., Deliane, F., Foulc, M.-P., Mehdi, A. and Durrieu, M.-C. (2012) Altered nanofeature size dictates stem cell differentiation. *Journal of Cell Science*, **125**, 1217-1244. doi:10.1242/jcs.093229

[8] Oh, S., Brammer, K.S., Li, Y.S.J., Teng, D., Engler, A.J., Chien, S. and Jin, S. (2009) Stem cell fate dictated solely by altered nanotube dimension. *Proceedings of the National Academy of Sciences*, **106**, 2130-2135. doi:10.1073/pnas.0813200106

[9] Martinez Mìro, M. (2012) Topographical control and characterization of Al/Al_2O_3 nanowire coatings for improved osseointegration of implant materials. Ph.D. Thesis, Saarland University, Saarbrücken.

[10] Wu, J., Mao, Z., Tan, H., Han, L., Ren, T. and Gao, C. (2012) Gradient biomaterials and their influences on cell migration. *Interface Focus*, **2**, 337-355. doi:10.1098/rsfs.2011.0124

[11] Kunzler, T.P., Huwiler, C., Drobeka, T., Vörös, J. and

Spencer, N.D. (2007) Systematic study of osteoblast response to nanotopography by means of nanoparticle-density gradients. *Biomaterials*, **28**, 5000-5006. doi:10.1016/j.biomaterials.2007.08.009

[12] Wang, P.Y., Clements, L.R., Thissen, H., Jane, A., Tsai, W.B. and Voelcker, N.H. (2012) Screening mesenchymal stem cell attachment and differentiation on porous silicon gradients. *Advanced Functional Materials*, **22**, 3414-3424. doi:10.1002/adfm.201200447

[13] Walpole, A.R., Briggs, E.P., Karlsson, M., Palsgard, E. and Wilshaw, P.R. (2003) Nano-porous alumina coatings for improved bone implant interfaces. *Materialwissenschaft und Werkstofftechnik*, **34**, 1064-1068. doi:10.1002/mawe.200300707

[14] Veith, M., Sow, E., Werner, U., Petersen, C. and Aktas, O.C. (2008) The transformation of core/shell aluminium/alumina nanoparticles into nanowires. *European Journal of Inorganic Chemistry*, **33**, 5181-5184. doi:10.1002/ejic.200800890

[15] Veith, M., Lee, J., Miró, M.M., Akkan, C.K., Dufloux, C. and Aktas, O.C. (2012) Bi-phasic nanostructures for functional applications. *Chemical Society Reviews*, **41**, 5117-5130. doi:10.1039/c2cs15345a

[16] Veith, M., Lee, J., Schmid, H. and Aktas, C. (2013) Ultra-rapid growth of biphasic nanowires in micro- and hypergravity. *Small*, **9**, 1042-1046. doi:10.1002/smll.201201833

